Electronic supplementary information (ESI)

Ethanol Synthesis via Catalytic CO_2 Hydrogenation over Multi-Elemental KFeCuZn/ZrO_2 Catalysts

Pengfei Du [a], Abdellah Ait El Fakir [a]*, Shirun Zhao,[a] Nazmul Hasan MD Dostagir,[a] HongLi Pan,[a] Kah Wei Ting,[a] Shinya Mine,[b] Yucheng Qian [a], Ken-ichi Shimizu,[a]* Takashi Toyao[a]*

[a] Institute for Catalysis, Hokkaido University, N-21, W-10, Sapporo 001-0021, Japan

[b] National Institute of Advanced Industrial Science and Technology (AIST), Research Institute for Chemical Process Technology, 4-2-1 Nigatake, Miyagino, Sendai 983-8551, Japan

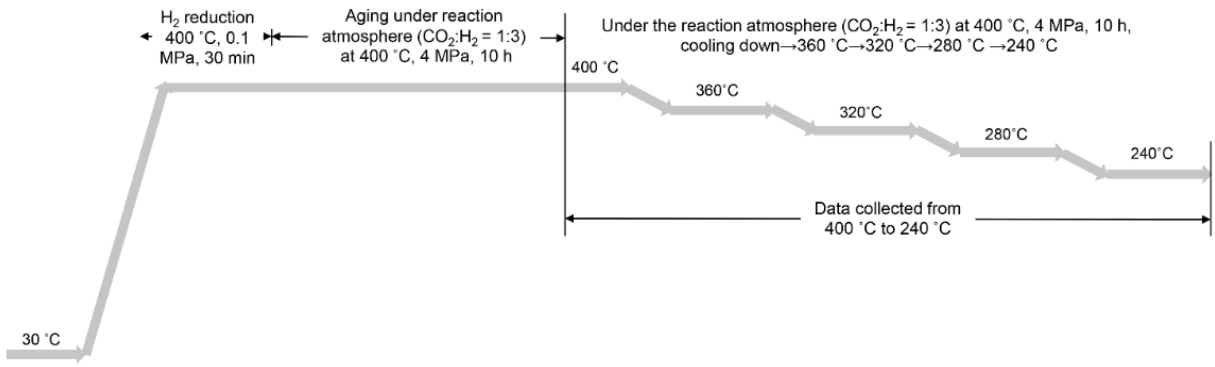

Figure S1. Typical experimental procedure for catalytic tests. After conducting H_2 reduction pre-treatment at 400 °C, accelerated aging treatment was performed at 400 °C in the reaction gas atmosphere. The catalytic performance at temperatures ranging from 400 °C to 240 °C was then recorded.

Table S1. Catalytic performances for CO_2 hydrogenation to form ethanol in this work and literature.

Catalyst	T (°C)	P (MPa)	WHSV (L g_{cat}^{-1} h^{-1})	CO_2 Conversion (%)	CO selectivity (%)	EtOH selectivity (%)	STY_{EtOH} (mmol g_{cat}^{-1} h^{-1})	References
$KFeCuZn/ZrO_2$*	320	4	12	39.1	17.8	14.6	3.5	This work
$KFeCuZn/ZrO_2$*	360	4	12	52.5	9.6	16.5	5.4	This work
$Na\text{-}Co/SiO_2$	250	5	6	21	27	6	0.5	[1]
$Cs\text{-}Cu_{0.8}Fe_{1.0}Zn_{1.0}$	330	5	4.5	35	20	12	1.1	[2]
Na-ZnFe@C	320	5	9	38.4	7.6	20.3	3.4	[3]
K/Cu-Zn-Fe	300	7	5	44.2	5.9	19.5	2.3	[4]
$K{-}In/Ce{-}ZrO_2$	300	10	4.5	19	57	5 (C_{2+})	0.4 (C_{2+})	[5]
$2K20Fe5Rh/SiO_2$	250	7.5	7	18	5	16	0.4	[6]
4.6K/CuMnZnFe	320	5	6	30.4	30.6	~7	1.7	[7]
$RhFeLi/TiO_2$	250	3	6000 h^{-1}	15.7	12.5	35.8	~1.3 (mmol · L_{cat}^{-1} · h^{-1})	[8]
$Co/La_4Ga_2O_9$	280	3	3	9.6	10.8	23.3	0.2	[9]
Pd/Fe_3O_4	300	0.1	60	0.3	0	97.5	0.4	[10]
Pd/CeO_2	240	3	3	9.2		99.2	1.2	[11]
Na-Rh@S-1	250	5	6	10	32	16	0.6	[12]
2%Na-Fe@C/5%KCuZnAl	320	5	4.5	39.2	9.4	35	3.6	[13]
$Li\text{-}Rh/SiO_2$	240	5	6	7	15.7	18.4	0.4	[14]
$Mo_1Co_1K_{0.6}$	320	5	3	23.5	77.2	8.9	0.1	[15]
K-CuMgZnFe/CZA	320	5	6	42.3	13.8	~17.4 (C_{2+})	~2.4 (C_{2+})	[16]
FeNaS-0.6	320	3	8	32.0	20.7	15.9 (C_{2+})	1.7 (C_{2+})	[17]
Cu/CeO_2	190	0.1	9	~0.1	~3	84	0.02	[18]
$Pd_2Ce@Si$	240	3	3	6	~2	94	0.8	[19]
$Co_2C{-}CuZnAl$	250	5	12	21	12.5	~18.9	~2.2	[20]
PdFe-6.9(37nm)	320	5	6	35.6	20.7	18.2 (C_{2+})	~1.9 (C_{2+})	[21]
$CuZnFe_{0.5}K_{0.15}$	300	6	5000 h^{-1}	42.3	49.2	36.7 (C_{2+})	3.4 (C_{2+})	[22]
Cu/Co_3O_4-2h	250	3	36	13.9	6.5	15.2	1.9	[23]
Rh-VO_x /MCM-4	250	3	6000 h^{-1}	12.1	20.1	24.1	1.1	[24]
Cu@Na-Beta	300	1.3	12	7.9	30.5	69.5	3.4	[25]
90Fe10Co (1.0)K	240	1.2	1.5	14.5	45.5	10.8	0.07	[26]
$Cu_{25}Fe_{22}Co_3K_3\text{-}CuZn_{1.0}K_{0.15}$	350	6	5000 h^{-1}	32.4	45.3	< 12	< 0.6 (mmol · L_{cat}^{-1} · h^{-1})	[27]
CoMoS	340	10.4	0.43	32	57.5	12.9	0.07	[28]
Na–CuCo-9	330	4	5	20.1	26.5	18.0	~2.3	[29]
$K\text{-}CuZnAl/Zr_{(0.03)}\text{-}CuFe$	320	4	24	28.8	~13.4	19.7 (C_{2+})	3.8 (C_{2+})	[30]
$Rh\text{-}Fe/TiO_2$	270	2	8	9.2	28.4	6.4	0.6	[31]
$Rh\text{-}Fe/SiO_2$	260	5	6	16.7	19.7	16	1.4	[32]
$IrMo\text{-}SiO_2$	200	4.9	2000 h^{-1}	7	41.7	4.3	0.04	[33]
$Rh/CeO_2\text{-}SiO_2$	240	5	3	8.3	33.5	6.1 (C_{2+})	0.2 (C_{2+})	[34]
RhLi/Y	250	3	6	13.1	86.6	2.7(C_{2+})	0.8 (C_{2+})	[35]
α-$CoMoO_4$/K	250	3	1.2	7.2	27.8	4.8 (C_{2+})	0.2 (C_{2+})	[36]
β-MoC_y	200	2	9	6	39	3 (C_{2+})	0.1 (C_{2+})	[37]
Pt/Co_3O_4	200	2	3	27	0	4.2 (C_{2+})	0.3 (C_{2+})	[38]
$In_2O_3{-}Fe_2O_3{-}K{-}Al_2O_3$	300	2	4	36	~40	42 (C_{2+})	3.02 (C_{2+})	[39]
3KCuFeZn/CuZnAlZr	300	5	3	27	28	24.6 (C_{2+})	0.9 (C_{2+})	[40]

*For the efficient evaluation of catalyst durability, accelerated aging treatment at 400 °C for 10 h was performed before the reaction.

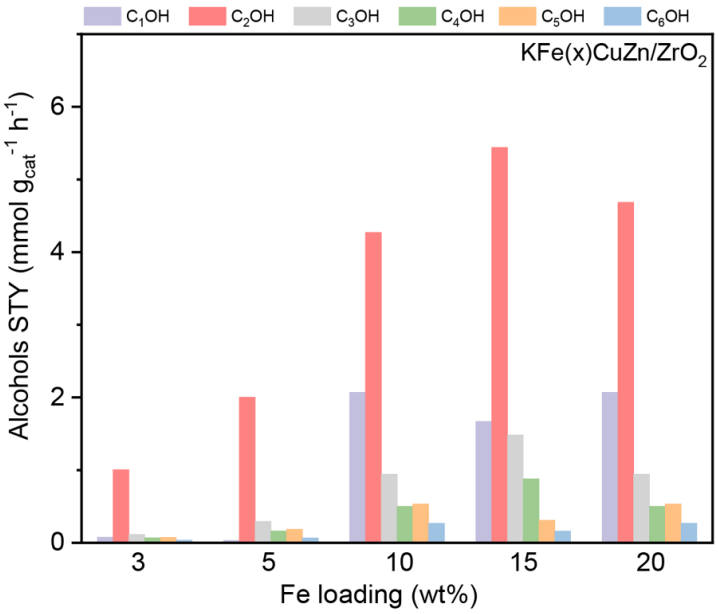

Figure S2. Alcohols STY distribution over the catalysts with different Fe loading at 360 °C. Conditions: 0.2 g catalyst, H_2: CO_2 = 3:1, and internal standard gas: Ar (0.8 vol%), 4 MPa, and 12 L g_{cat}^{-1} h^{-1}.

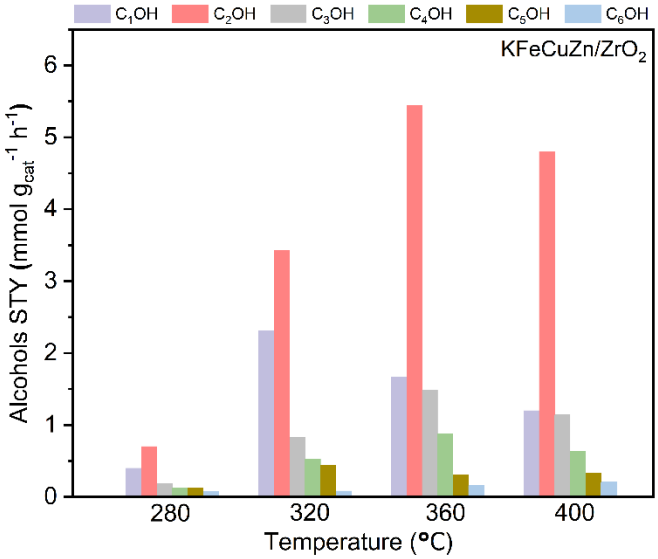

Figure S3. Alcohols STY distribution at 280–400°C. Conditions: 0.2 g catalyst, H_2: CO_2= 3:1, and internal standard gas: Ar (0.8 vol%), 4 MPa, and 12 L g_{cat}^{-1} h^{-1}.

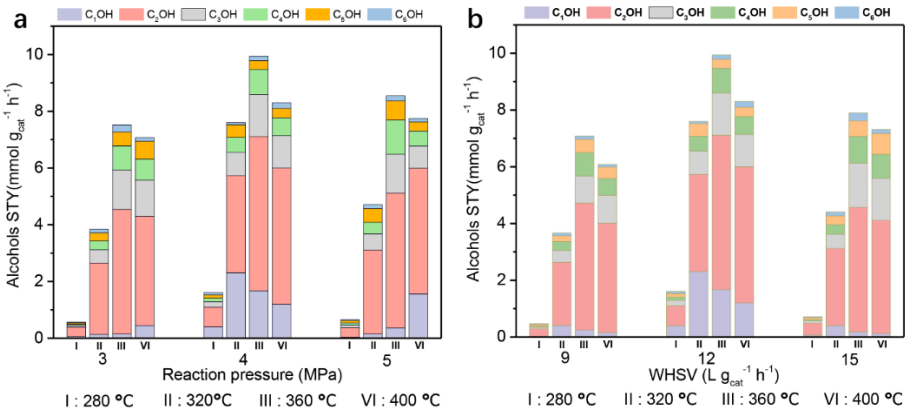

Figure S4. Influence of pressure (a) and gas hourly space velocity (GHSV, b) on alcohols STY at 280-400 °C. Conditions: 0.2 g catalyst, H_2:CO_2 = 3:1, and internal standard gas : Ar (0.8 vol%), 3-5 MPa, and 9-15 L g_{cat}^{-1} h^{-1}.

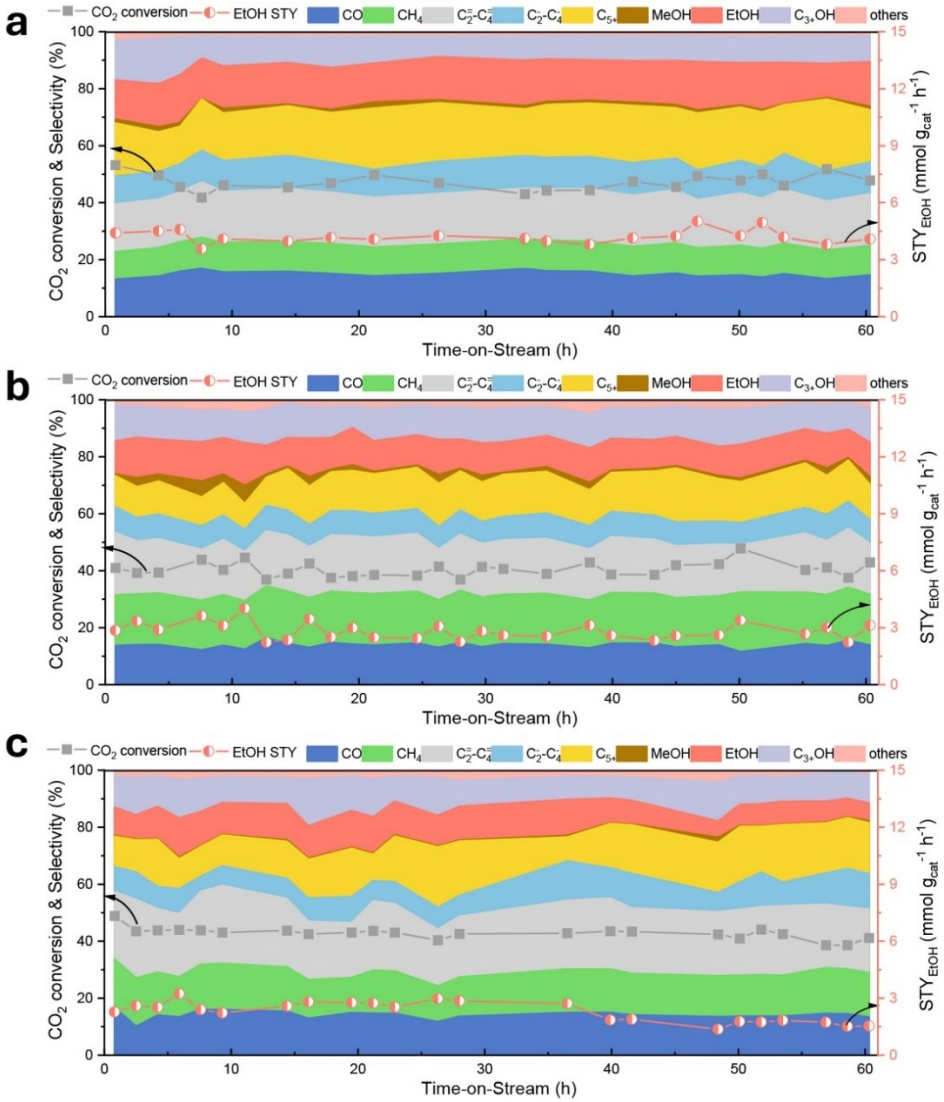

Figure S5. Stability test for KFeCu/ZrO_2 KFeZn/ZrO_2 and KFe/ZrO_2 at 360 °C. Pretreatment condition: 400 °C, 0.1 MPa, H_2/Ar (99/1%), and 0.5 h. Reaction condition: 12 L g_{cat}^{-1} h^{-1}, 4.0 MPa, and H_2/CO_2/Ar (74.4/24.8/0.8%). Ar was used as an internal standard gas. Accelerated aging treatment was performed before reaction at 400°C for 10 h under the reaction environment. Others include acetaldehyde and ethyl formate. In Figure S5, the gray dots are CO_2 conversion; red dot is EtOH STY.

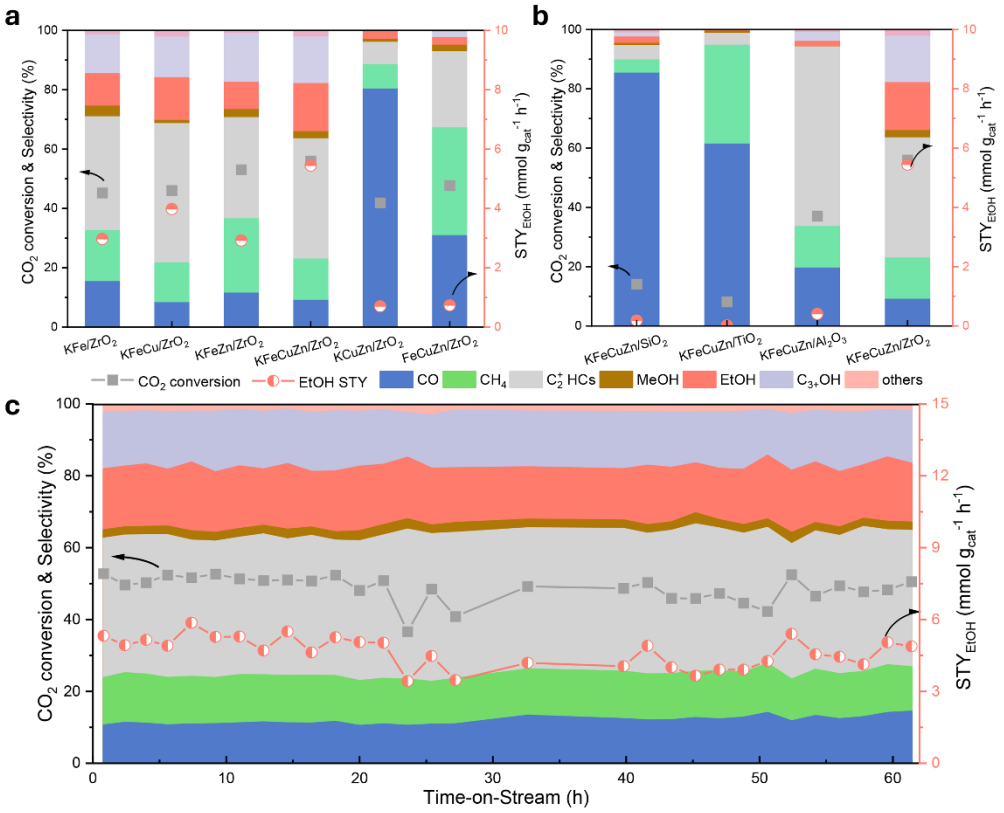

Figure S6. Simplified exhibition for catalytic performance. (a) CO_2 conversion and product selectivity at 360 °C and STY_{EtOH} over KFe/ZrO_2 based catalysts; (b) CO_2 conversion, product selectivity, and STY_{EtOH} over different supporting; and (c) stability test for $KFeCuZn/ZrO_2$ at 360 °C. Pretreatment condition: 400 °C, 0.1 MPa, H_2 (99%), and 0.5 h. Reaction condition: 12 L g_{cat}^{-1} h^{-1}, 4.0 MPa, and $H_2/CO_2/Ar$ (74.4/24.8/0.8%). Ar was used as an internal standard gas. The data was collected after 3 h, when the temperature and rection were stable. Accelerated aging treatment was performed before reaction at 400°C for 10 h under the reaction environment. HCs: hydrocarbons; Others include acetaldehyde and ethyl formate. In Figure S6 a and b, the gray dot is CO_2 conversion; red dot is EtOH STY.

Table S2. Specific surface areas and pore volumes of studied KFe-based catalysts.

Samples	BET specific surface area (m^2/g)	Pore volume (cm^3/g)
KFe/ZrO_2	60.4	0.059
$KFeCu/ZrO_2$	54.8	0.051
$KFeZn/ZrO_2$	41.4	0.039
$KFeCuZn/ZrO_2$	40.6	0.036

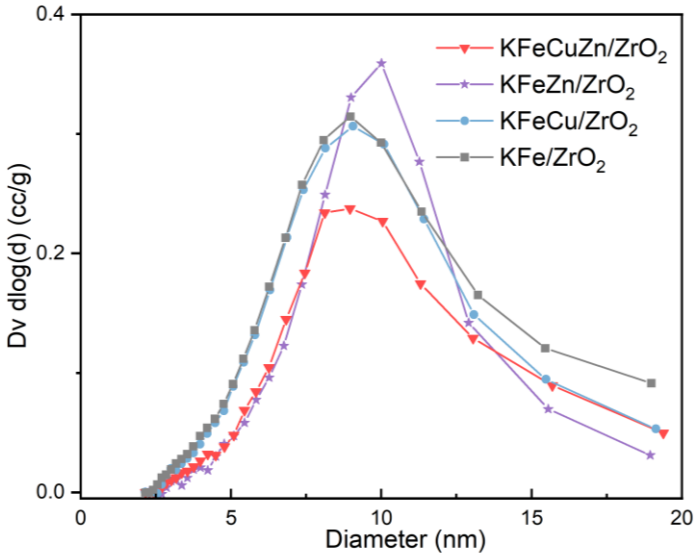

Figure S7. Pore size distribution curve of the studied samples calculated from desorption branch of the isotherm by the BJH method.

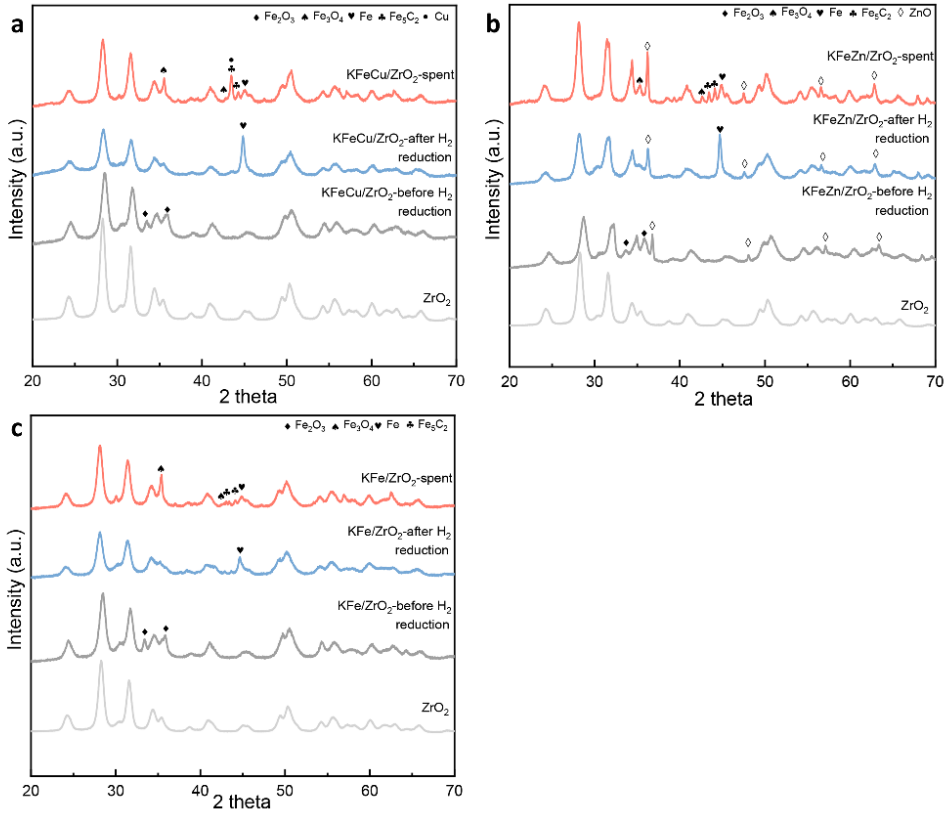

Figure S8. XRD patterns for (a) KFe/CuZrO$_2$; (b) KFeZn/ZrO$_2$; (c) KFe/ZrO$_2$ before and after H$_2$ reduction, as well as after reaction. “Spent catalyst" refers to a sample that has undergone a 20-hour accelerated aging treatment at 400 °C under the reaction condition.

Table S3. Curve-fitting results of the *ex situ* Fe *K*-edge FT-EXAFS spectra of the KFeCuZn/ZrO_2 catalyst.

Sample	shell	CN	R (Å)	σ^2 (Å^2)	ΔE	R factor
KFeCuZn/ZrO_2-before H_2 reduction	Fe–O	4.4±0.7	1.99±0.01	0.007	2.43	0.014
	Fe–O–Fe	4.6±0.9	2.98±0.01	0.008		
KFeCuZn/ZrO_2- after H_2 reduction	Fe–Fe	5.8±2.1	2.45±0.02	0.005	0.85	0.008
	Fe–Fe	4.8±2.2	2.83±0.01	0.005		
KFeCuZn/ZrO_2-spent	Fe–O(C)	3	1.99±0.02	0.003	8	0.017
	Fe–C(O)	2.7±1.1	1.87±0.01	0.003		
	Fe–C–Fe	3.9±0.3	2.58±0.01	0.01		
	Fe–C–Fe	1.1±0.6	2.40±0.02	0.008		
	Fe–O–Fe	5.6±1.2	3.42±0.01	0.01		

CN: coordination numbers; R: bond distance; σ^2: Debye-Waller factors; R factor: goodness of fit. S_0^2 was set to 0.8, according to the EXAFS fit of Fe foil.

Table S4. Curve-fitting results of the *ex situ* Cu *K*-edge FT-EXAFS spectra of the KFeCuZn/ZrO_2 catalyst.

Sample	shell	CN	R (Å)	σ^2 (Å^2)	ΔE	R factor
KFeCuZn/ZrO_2- before H_2 reduction	Cu–O	3.9±0.5	1.93±0.005	0.005	5.2	0.019
	Cu–O–Cu	2.0±0.4	2.91±0.013	0.008		
KFeCuZn/ZrO_2- after H_2 reduction	Cu–Cu	8.9±1.2	2.54±0.004	0.009	4.42	0.014
KFeCuZn/ZrO_2-spent	Cu–Cu	10.4±1.1	2.54±0.007	0.009	4.57	0.014

CN: coordination numbers; R: bond distance; σ^2: Debye-Waller factors; R factor: goodness of fit. S_0^2 was set to 0.87, according to the EXAFS fit of Cu foil.

Table S5. Curve-fitting results of the *ex situ* Zn *K*-edge FT-EXAFS spectra of the KFeCuZn/ZrO_2 catalyst.

Sample	shell	CN	R (Å)	σ^2 (Å^2)	ΔE	R factor
KFeCuZn/ZrO_2- before H_2 reduction	Zn–O	3.2±0.01	1.95±0.005	0.005	1.6	0.018
	Zn–O–Zn	8.3±0.01	3.22±0.013	0.010		
KFeCuZn/ZrO_2- after H_2 reduction	Zn–O	2.8±0.8	3.22±0.02	0.004	1.2	0.04
	Zn–Zn	1.2±0.8	2.58±0.05	0.01		
KFeCuZn/ZrO_2-spent	Zn–O–Zn	11±1.5	3.22±0.02	0.01		
	Zn–O	3.1±0.6	3.22±0.01	0.004	1.6	0.03
	Zn–O–Zn	10.8±1.1	3.22±0.01	0.01		

CN: coordination numbers; R: bond distance; σ^2: Debye-Waller factors; R factor: goodness of fit. S_0^2 was set to 0.96, according to the EXAFS fit of Zn foil.

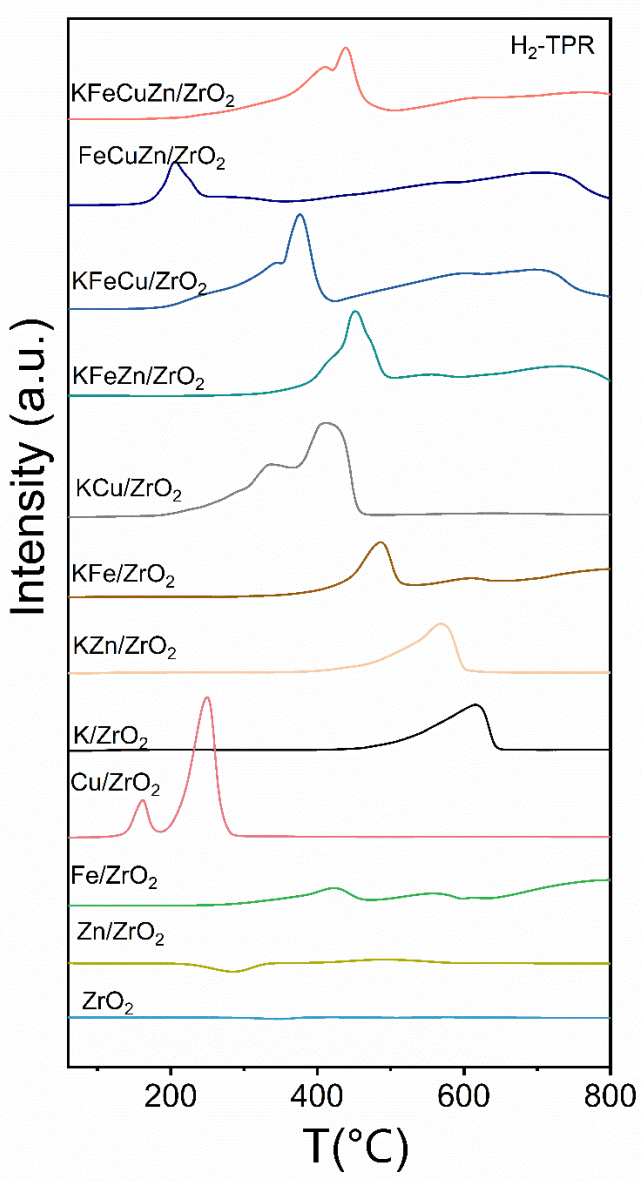

Figure S9. H_2-TPR results over different control catalysts. Condition: Ar pretreatment at 200 °C for 1hr, heating in 10% H_2/Ar from 50 to 800 °C.

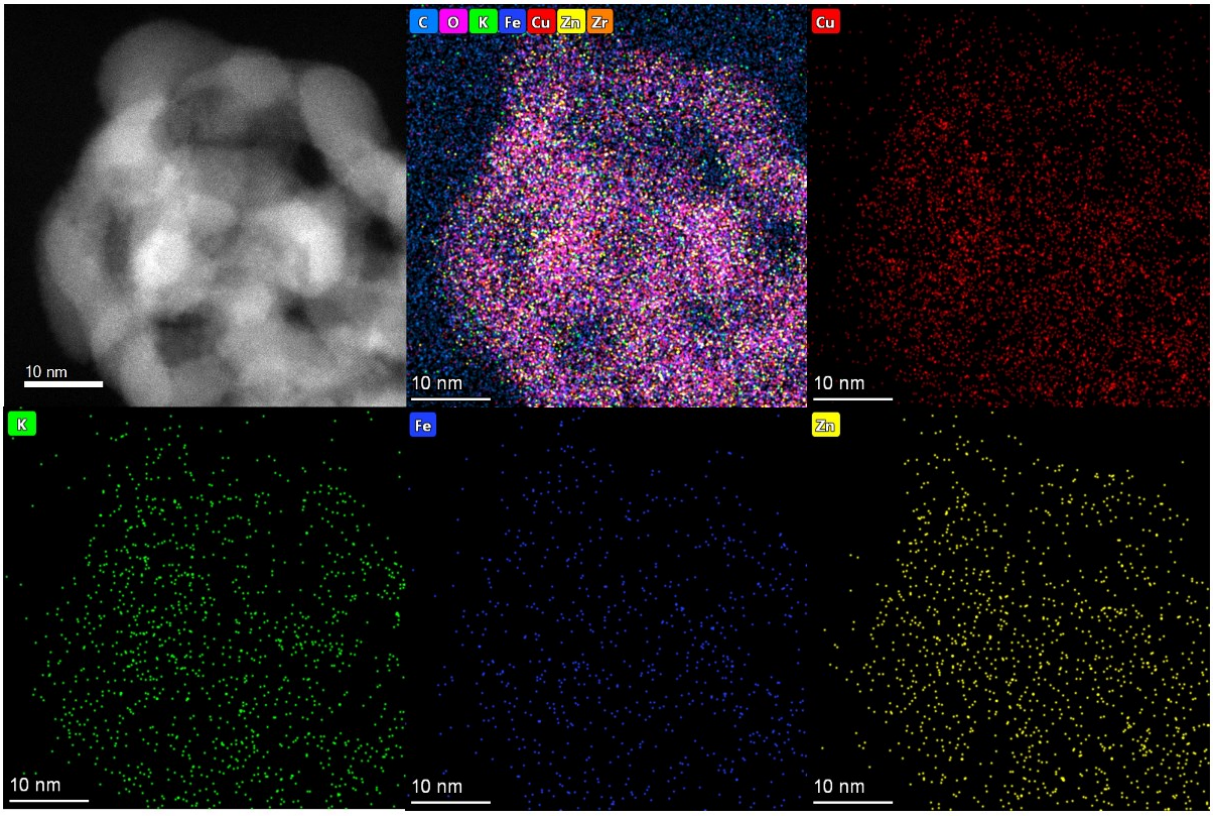

Figure S10. HAADF-STEM image and corresponding EDS mapping images of the fresh KFeCuZn/ZrO_2 that has undergone H_2 reduction pretreatment at 400 °C.

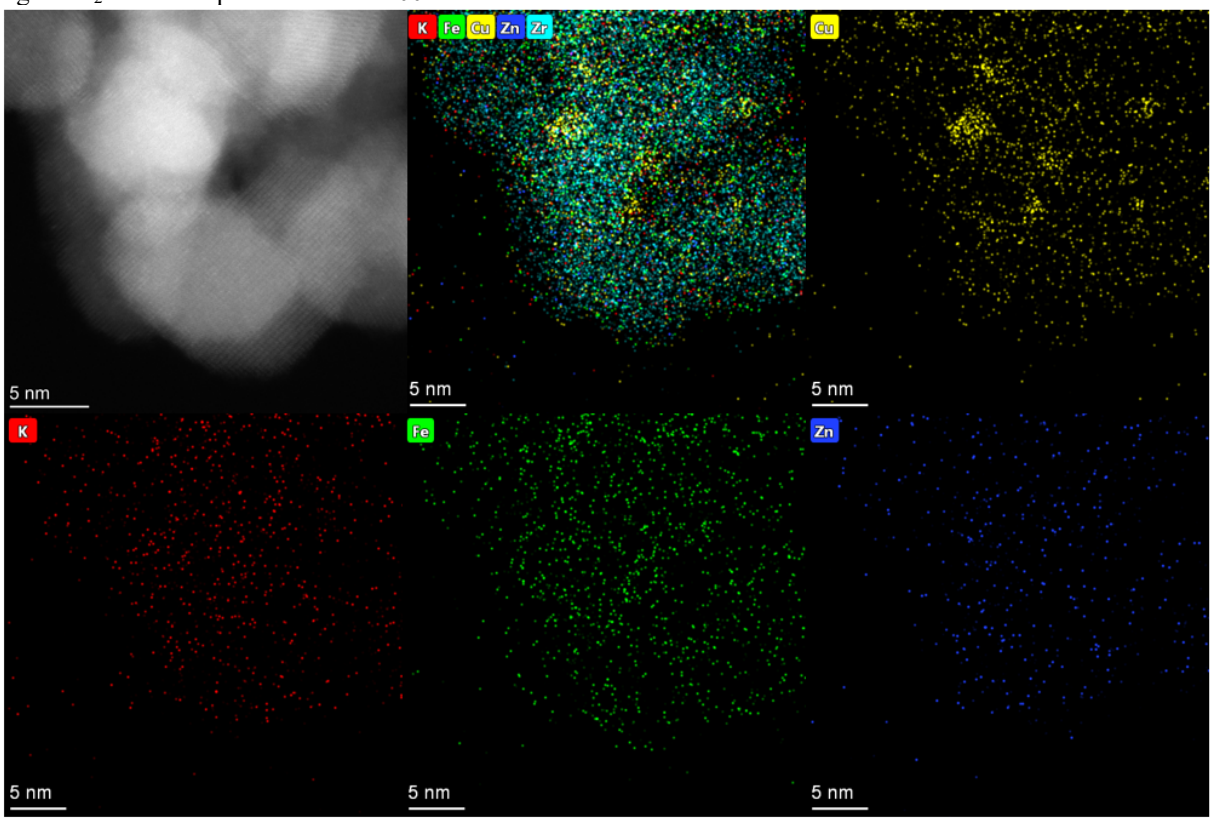

Figure S11. HAADF-STEM image and corresponding EDS mapping images of the spent KFeCuZn/ZrO_2 that has undergone a 20-hour accelerated aging treatment at 400 °C under the reaction condition.

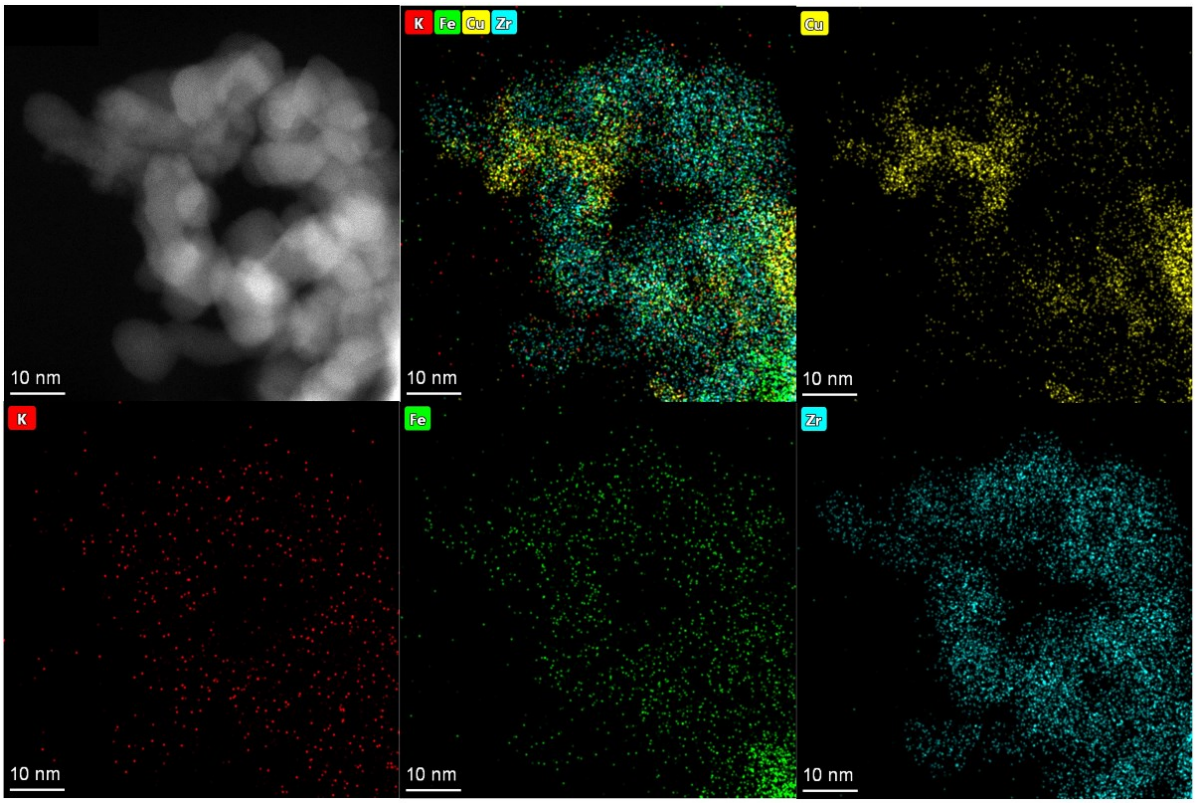

Figure S12. HAADF-STEM image and corresponding EDS mapping images of the spent KFeCu/ZrO_2 that has undergone a 20-hour accelerated aging treatment at 400 °C under the reaction condition.

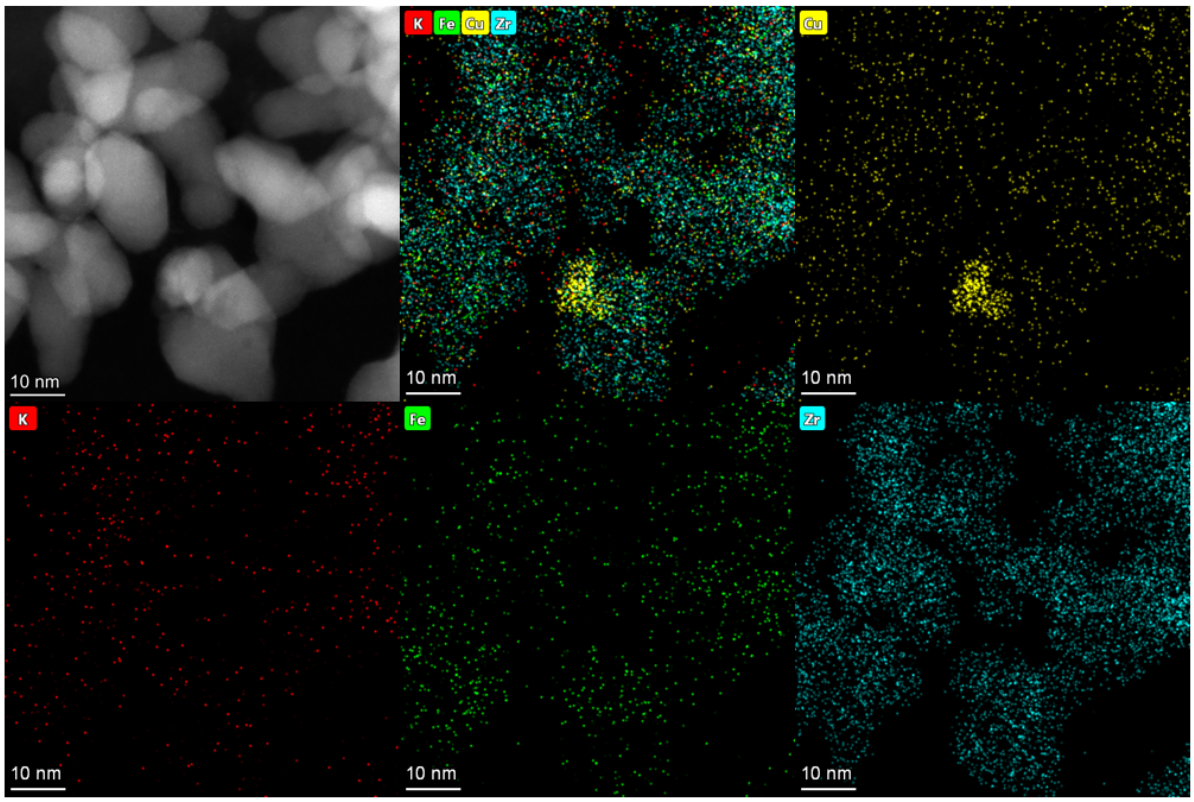

Figure S13. HAADF-STEM image and corresponding EDS mapping images of the spent KFeCu/ZrO_2 that has undergone a 20-hour accelerated aging treatment at 400 °C under the reaction condition.

Table S6. DRIFTS peak assignments of the surface species for CO_2 hydrogenation.

Surface species	Wavenumber (cm^{-1})	References
*CO_3	1227–1281	2
*HCO_3	1620-1640	41
*CH_3O	2826, 1070, 2940, 2841-2866	42
*HCOO	2676–2774, 1593–1610, 1337–1397	2,43
*CH_3CH_2O	2856, 2928, 2963, 1458,1095	25,44
*CH_3CHO	1415, 1340, 1720	2,44
CH_4	3016	2
CO (gas)	2110, 2179	44
Linear–CO	2060–2098	44
Bridging–CO	1900–1940	44

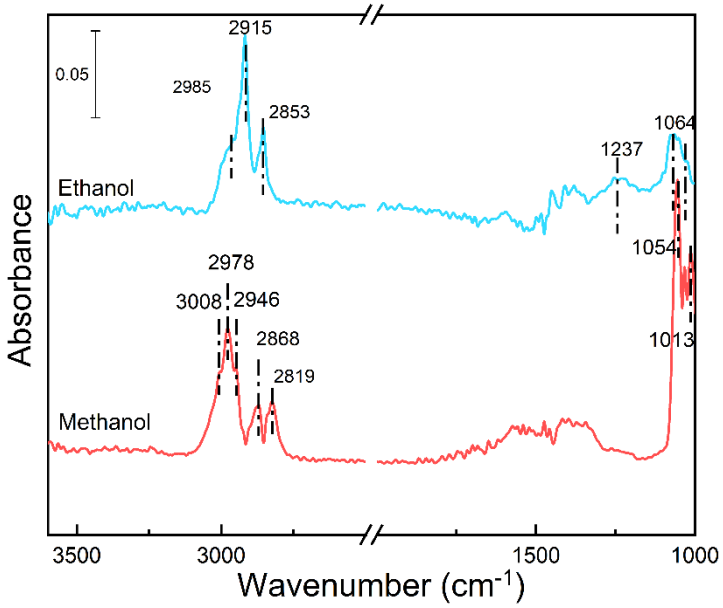

Figure S14. *In situ* DRIFTS spectra of methanol and ethanol adsorption on spent KFeCuZn/ZrO_2.

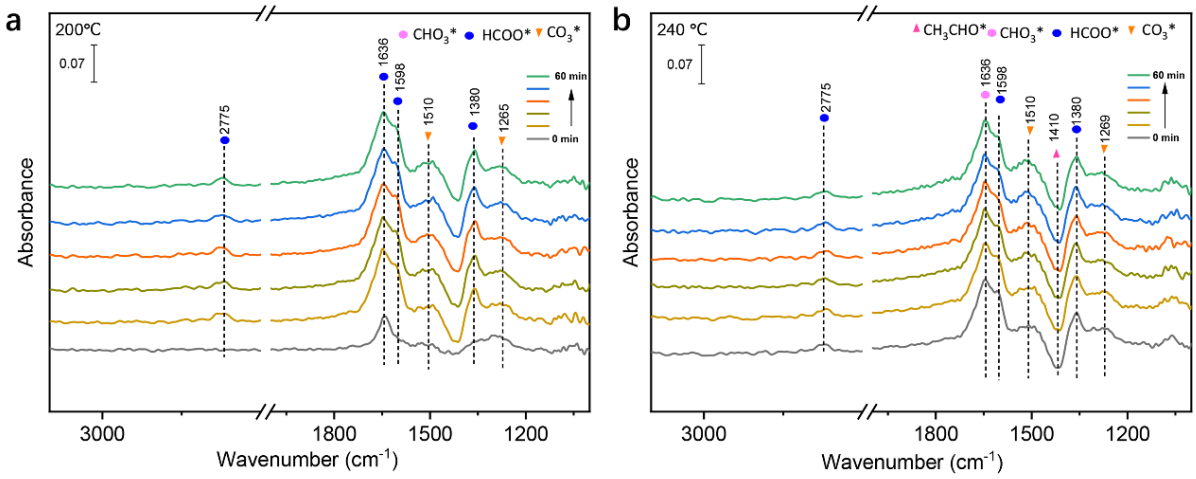

Figure S15. *In situ* DRIFTS spectra of the CO_2 + H_2 reaction over the KFeCuZn/ZrO_2 catalyst taken under 0.5 MPa CO_2/H_2 flow at different reaction temperature (a: 200 °C; b: 240 °C).

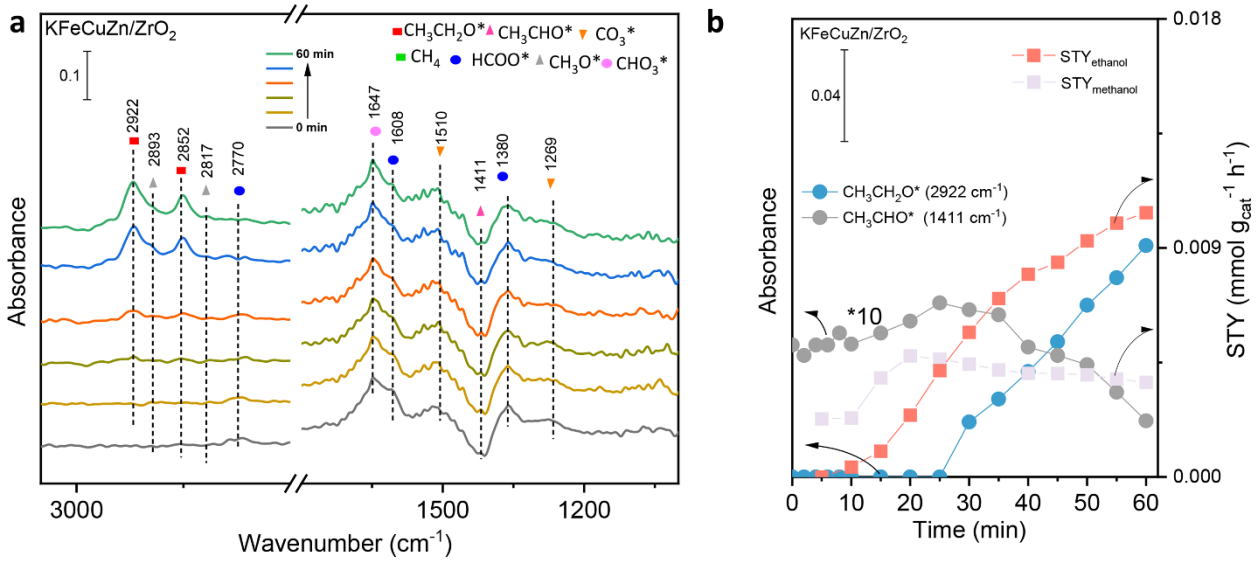

Figure S16. *In situ* DRIFTS spectra. (a) The time resolution spectra of the CO_2 + H_2 reaction over the KFeCuZn/ZrO_2 at 280 °C; (b) Dynamic IR peak intensities of CH_3CHO* (1411 cm^{-1}) and CH_3CH_2O* (2922 cm^{-1}) and some of products (ethanol and methanol) amount from micro-GC at 280 °C.

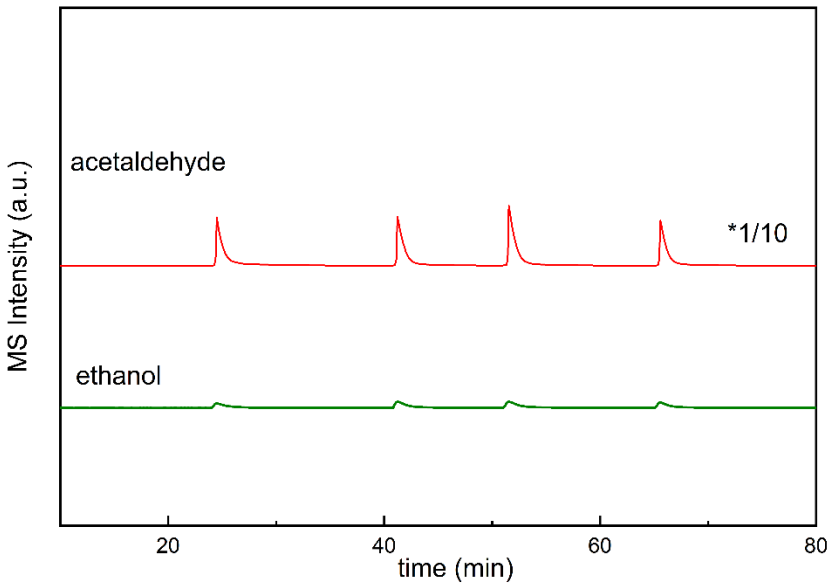

Figure S17. Pulse experiment over the spent KFeCuZn/ZrO_2 catalyst taken under 0.1 MPa CO_2/H_2 flow at 320 °C.

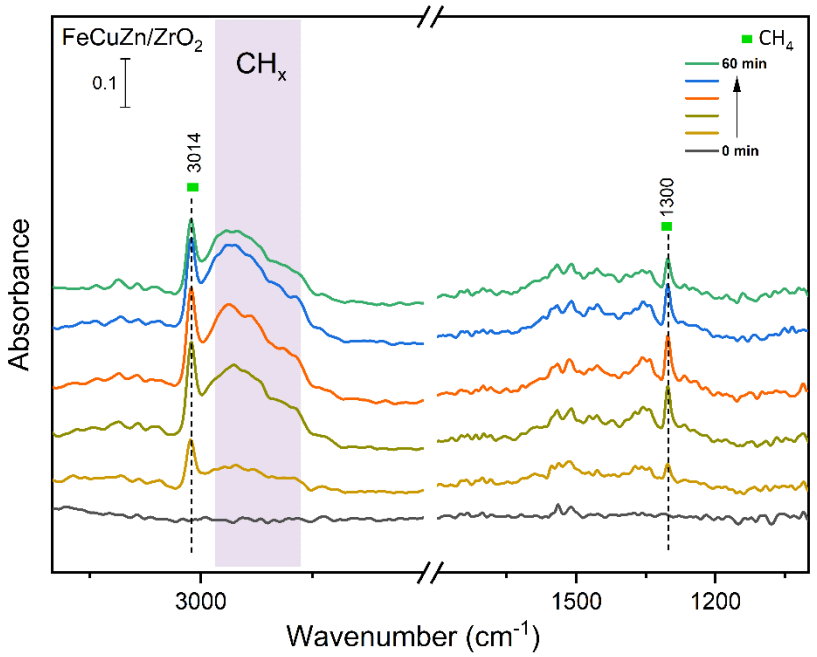

Figure S18. *In situ* DRIFTS spectra of the CO_2 + H_2 reaction over the FeCuZn/ZrO_2 catalyst taken under 0.5 MPa CO_2/H_2 flow at 320 °C.

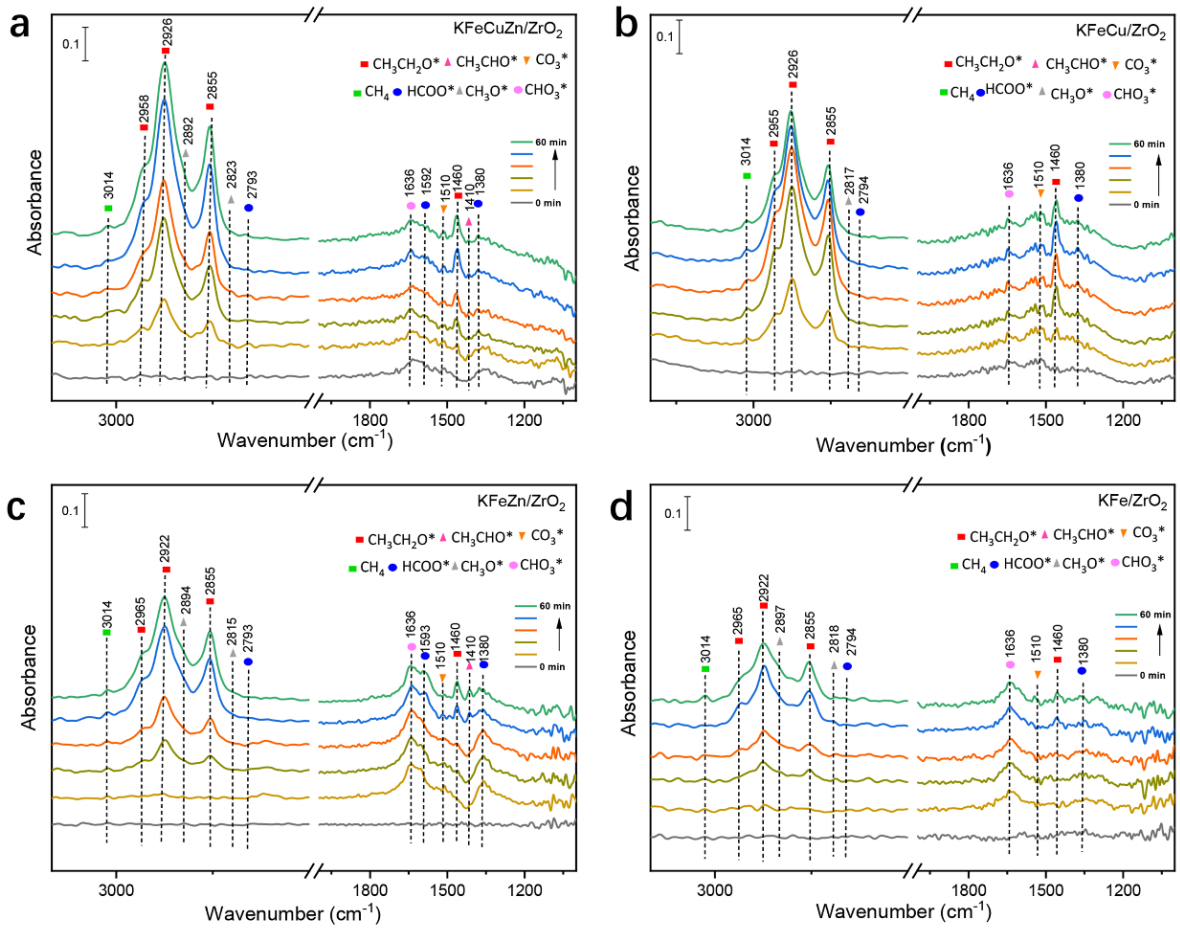

Figure S19. *In situ* DRIFTS spectra of the CO_2 + H_2 reaction over the KFeCuZn/ZrO_2 (a), KFeCu/ZrO_2 (b), KFeZn/ZrO_2 (c), and KFe/ZrO_2 (d), catalyst taken under 0.5 MPa CO_2/H_2 flow at 320 °C.

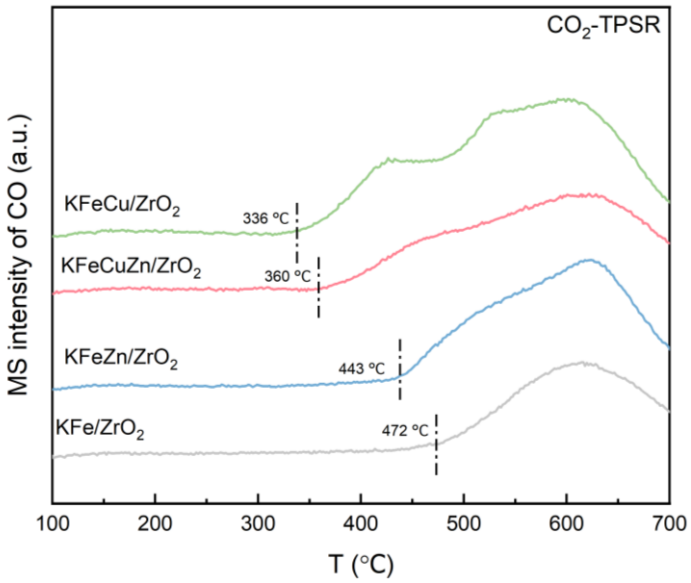

Figure S20. MS signals of m/z=28 in CO_2-TPSR after CO_2 pre-adsorbed catalysts under 5%H_2/Ar flow, over KFeZnCu/ZrO_2, KFeZn/ZrO_2, KFeCu/ZrO_2, and KFe/ZrO_2.

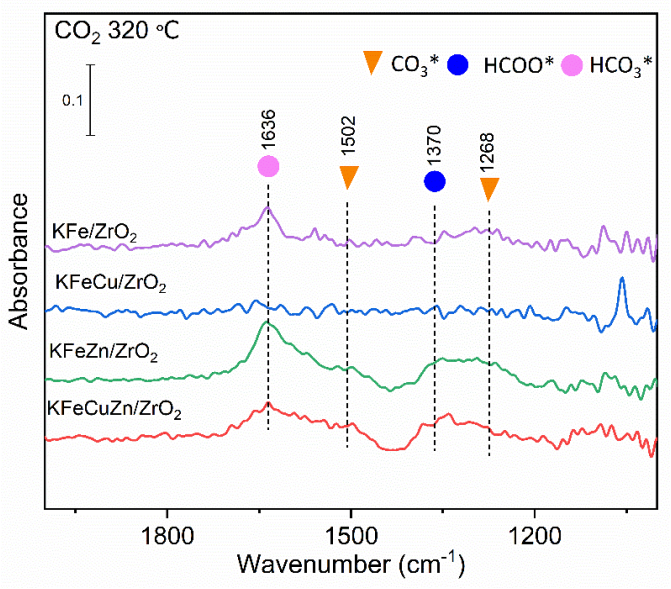

Figure S21. *In situ* DRIFTS spectra of the CO_2 adsorption over the different catalysts, taken under 0.5 MPa at 320 °C.

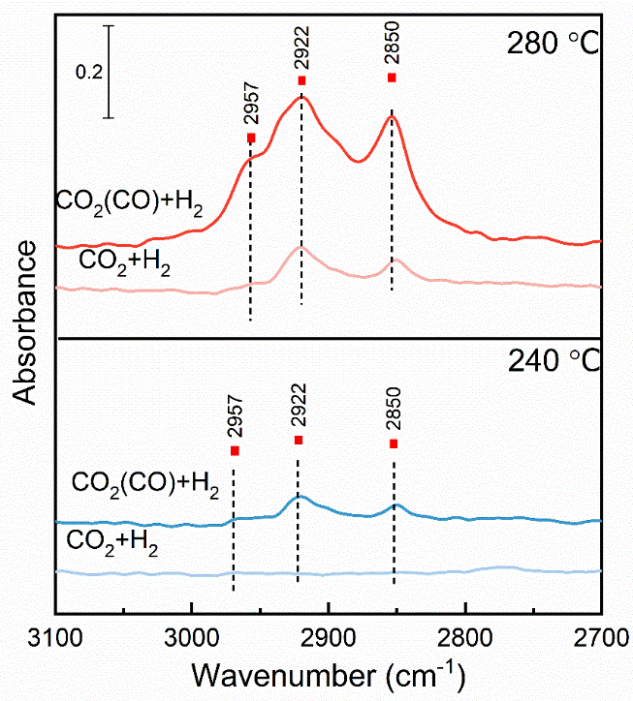

Figure S22. *In situ* DRIFTS spectra of the $CO_2 + H_2$ and CO co-feeding (20%CO in CO_x) reactions over the KFeCuZn/ZrO_2 catalyst taken under 0.5 MPa at 240 and 280 °C.

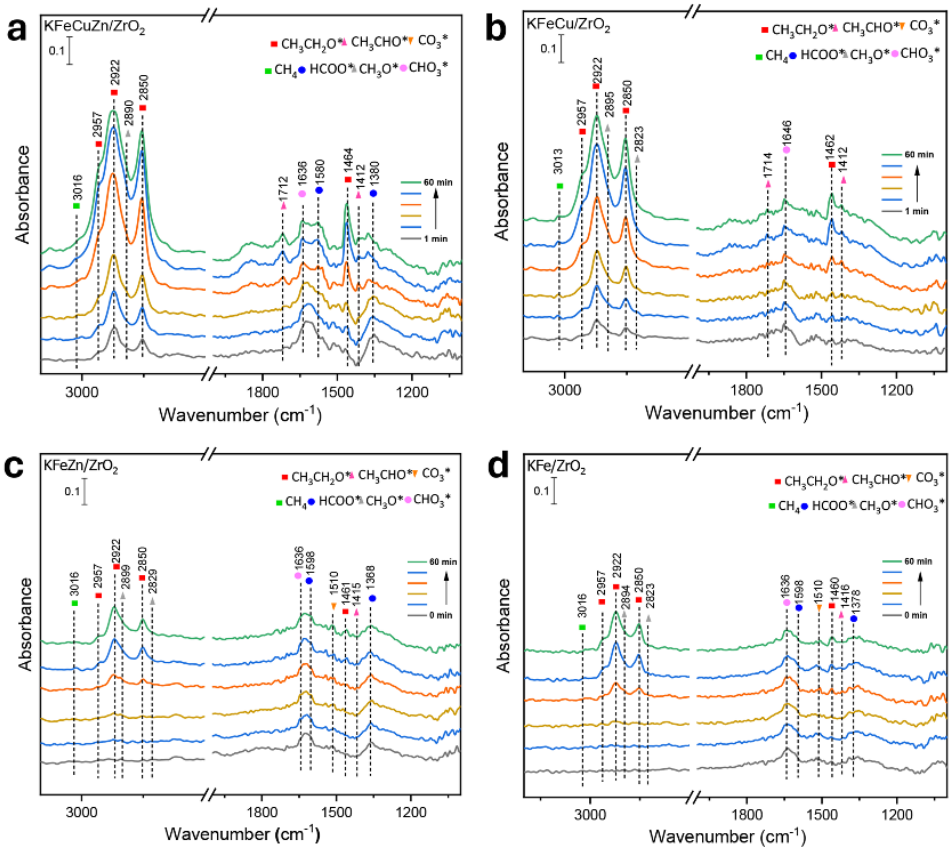

Figure S23. *In situ* DRIFTS spectra of the CO + H_2 reaction over the KFeCuZn/ZrO_2 (a), KFeCu/ZrO_2 (b), KFeZn/ZrO_2 (c), and KFe/ZrO_2 (d), catalyst taken under 0.5 MPa at 280 °C.

Notes and references:

1 S. Zhang, Z. Wu, X. Liu, Z. Shao, L. Xia, L. Zhong, H. Wang and Y. Sun, *Appl. Catal., B*, 2021, **293**, 120207.

2 D. Xu, M. Ding, X. Hong, G. Liu and S. C. E. Tsang, *ACS Catal*, 2020, **10**, 5250–5260.

3 Y. Wang, W. Wang, R. He, M. Li, J. Zhang, F. Cao, J. Liu, S. Lin, X. Gao, G. Yang, M. Wang, T. Xing, T. Liu, Q. Liu, H. Hu, N. Tsubaki and M. Wu, *Angewandte Chemie International Edition*, 2023, **62**, e20231178.

4 M. Takagawa, A. Okamoto, H. Fujimura, Y. Izawa and H. Arakawa, *Stud. Surf. Sci. Catal.*, 1998, **114**, 525–528.

5 X. Xi, F. Zeng, H. Zhang, X. Wu, J. Ren, T. Bisswanger, C. Stampfer, J. P. Hofmann, R. Palkovits and H. J. Heeres, *ACS Sustain. Chem. Eng.*, 2021, **9**, 6235–6249.

6 A. Goryachev, A. Pustovarenko, G. Shterk, N. S. Alhajri, A. Jamal, M. Albuali, L. van Koppen, I. S. Khan, A. Russkikh, A. Ramirez, T. Shoinkhorova, E. J. M. Hensen and J. Gascon, *ChemCatChem*, 2021, **13**, 3324–3332.

7 D. Xu, M. Ding, X. Hong and G. Liu, *ACS Catal.*, 2020, **10**, 14516–14526.

8 C. Yang, R. Mu, G. Wang, J. Song, H. Tian, Z. J. Zhao and J. Gong, *Chem. Sci.,* 2019, **10**, 3161–3167.

9 K. An, S. Zhang, J. Wang, Q. Liu, Z. Zhang and Y. Liu, *J. Energy Chem.*, 2021, **56**, 486–495.

10 F. J. Caparrós, L. Soler, M. D. Rossell, I. Angurell, L. Piccolo, O. Rossell and J. Llorca, *ChemCatChem*, 2018, **10**, 2365–2369.

11 Y. Lou, F. jiang, W. Zhu, L. Wang, T. Yao, S. Wang, B. Yang, B. Yang, Y. Zhu and X. Liu, *Appl Catal B*, 2021, **291**, 120122.

12 F. Zhang, W. Zhou, X. Xiong, Y. Wang, K. Cheng, J. Kang, Q. Zhang and Y. Wang, *J. Phys. Chem. C*, 2021, **125**, 24429–24439.

13 Y. Wang, K. Wang, B. Zhang, X. Peng, X. Gao, G. Yang, H. Hu, M. Wu and N. Tsubaki, *ACS Catal.*, 2021, **11**, 11742–11753.

14 H. Kusama, K. Okabe, K. Sayama and H. Arakawa, *Catal. Today*, 1996, **28**, 261–266.

15 S. Liu, H. Zhou, L. Zhang, Z. Ma and Y. Wang, *Chem. Eng. Technol. 2*, 2019, **42**, 962–970.

16 D. Xu, H. Yang, X. Hong, G. Liu and S. C. Edman Tsang, *ACS Catal.*, 2021, **11**, 8978–8984.

17 R. Yao, J. Wei, Q. Ge, J. Xu, Y. Han, Q. Ma, H. Xu and J. Sun, *Appl. Catal., B* , 2021, **298**, 120556.

18 A. H. M. da Silva, L. H. Vieira, C. S. Santanta, M. T. M. Koper, E. M. Assaf, J. M. Assaf and J. F. Gomes, *Appl. Catal., B,* 2023, **324**, 122221.

19 J. Chen, Y. Zha, B. Liu, Y. Li, Y. Xu and X. Liu, *ACS Catal.*, 2023, **13**, 7110–7121.

20 S. Zhang, C. Huang, Z. Shao, H. Zhou, J. Chen, L. Li, J. Lu, X. Liu, H. Luo, L. Xia, H. Wang and Y. Sun, *ACS Catal.*, 2023, **13**, 3055–3065.

21 Y. Wang, Y. Zhou, X. Zhang, M. Wang, T. Liu, J. Wei, G. Zhang, X. Hong and G. Liu, *Appl. Catal., B*, 2024, **345**, 123691.

22 S. Li, H. Guo, C. Luo, H. Zhang, L. Xiong, X. Chen and L. Ma, *Catal. Lett.*, 2013, **143**, 345–355.

23 C. Yang, S. Liu, Y. Wang, J. Song, G. Wang, S. Wang, Z. Zhao, R. Mu and J. Gong, *Angew. Chem., Int. Ed.* , 2019, **131**, 11364–11369.

24 G. Wang, R. Luo, C. Yang, J. Song, C. Xiong, H. Tian, Z. J. Zhao, R. Mu and J. Gong, *Sci. China: Chem.*, 2019, **62**, 1710–1719.

25 L. Ding, T. Shi, J. Gu, Y. Cui, Z. Zhang, C. Yang, T. Chen, M. Lin, P. Wang, N. Xue, L. Peng, X. Guo, Y. Zhu, Z. Chen and W. Ding, *Chem*, 2020, **6**, 2673–2689.

26 M. K. Gnanamani, H. H. Hamdeh, G. Jacobs, W. D. Shafer, S. D. Hopps, G. A. Thomas and B. H. Davis, *ChemCatChem*, 2017, **9**, 1303–1312.

27 H. Guo, S. Li, F. Peng, H. Zhang, L. Xiong, C. Huang, C. Wang and X. Chen, *Chem. Lett.*, 2015, **145**, 620–630.

28 D. L. S. Nieskens, D. Ferrari, Y. Liu and R. Kolonko, *Catal. Commun.*, 2011, **14**, 111–113.

29 M. Irshad, H. J. Chun, M. K. Khan, H. Jo, S. K. Kim and J. Kim, *Appl. Catal., B*, 2024, **340**, 123201.

30 Q. Zhang, S. Wang, X. Shi, M. Dong, J. Chen, J. Zhang, J. Wang and W. Fan, *Appl. Catal., B*, 2024, **346**, 123748.

31 M. R. Gogate and R. J. Davis, *Catal. Commun.*, 2010, **11**, 901–906.

32 H. Kusama, K. Okabe, K. Sayama and H. Arakawa, *energy*, 1997, **22**, 343–348.

33 M. Kishida, K. Yamada, H. Nagata and K. Wakabayashi, *Chem. Lett.*, 1994, 555–556.

34 H. Kusama, K. Okabe, K. Sayama and H. Arakawa, *J. Jpn. Pet. Inst.*, 1999, **42**, 178–179.

35 K. Kitamura Bando, K. Soga, K. Kunimori and H. Arakawa, *Appl. Catal., A*, 1998, **175**, 67–81.

36 A. Calafat, F. Âtima Vivas, J. Ân, L. Brito, C. San, E. T. Âbal and V. Âchira, *Appl. Catal., A*, 1998, **172**, 217–224.

37 W. Xu, P. J. Ramirez, D. Stacchiola and J. A. Rodriguez, *Chem. Lett.*, 2014, **144**, 1418–1424.

38 B. Ouyang, S. Xiong, Y. Zhang, B. Liu and J. Li, *Appl. Catal., A*, 2017, **543**, 189–195.

39 D. Goud, S. R. Churipard, D. Bagchi, A. K. Singh, M. Riyaz, C. P. Vinod and S. C. Peter, *ACS Catal.*, 2022, **12**, 11118–11128.

40 Y. Wang, D. Xu, X. Zhang, X. Hong and G. Liu, *Catal. Sci. Technol.*, 2022, **12**, 1539–1550.

41 N. H. M. Dostagir, R. Rattanawan, M. Gao, J. Ota, J. Y. Hasegawa, K. Asakura, A. Fukouka and A. Shrotri, *ACS Catal.*, 2021, **11**, 9450–9461.

42 X. Chang, X. Han, Y. Pan, Z. Hao, J. Chen, M. Li, J. Lv and X. Ma, *Ind. Eng. Chem. Res.*, 2022, **61**, 6872–6883.

43 I. Ro, Y. Liu, M. R. Ball, D. H. K. Jackson, J. P. Chada, C. Sener, T. F. Kuech, R. J. Madon, G. W. Huber and J. A. Dumesic, *ACS Catal.*, 2016, **6**, 7040–7050.

44 T. Liu, D. Xu, M. Song, X. Hong and G. Liu, *ACS Catal.*, 2023, **13**, 4667–4674.